Trans Indian Inst Met (2022) 75(5):1153–1162
https://doi.org/10.1007/s12666-021-02471-8

ORIGINAL ARTICLE

Synthesis and Stability of Higher-Order Superstructure of Cubic Laves Phase in an Al-Cu-Ta alloy

T. P. Yadav[1] · Harshit Agarwal[1] · M. A. Shaz[1] · N. K. Mukhopadhyay[2]

Received: 22 September 2021 / Accepted: 8 November 2021 / Published online: 15 January 2022

Abstract In this work, we investigated on the synthesis and stability of a ternary complex metallic alloy in Al-Cu-Ta system, close to the composition of $Al_{56.6}Cu_{3.9}Ta_{39.5}$. The Rietveld refinement of X-ray diffraction data established its structure to be FCC (space group: $F\bar{4}3m$; lattice parameter, a = 45.339 (7) Å), which has been correlated with the seventh order superstructure (7x7x7) of imaginary cubic Laves phase (lattice parameter of it being close to 6.5 Å). After annealing at1400K for 24 h, the as-cast alloy exhibited the same type of intermetallic phase with the slightly reduced lattice parameter (a = 45.2908 (9)Å). However, no other major phases could be detected from the X-ray diffraction data in both the as-cast and annealed alloys. The microhardness tests showed a variation of hardness from 8.8 GPa to 7.2 GPa for annealed and 7.6 GPato 4.8 GPa for as-cast samples. The variation of hardness with load, known as indentation size effect, was found to be relatively less in the annealed sample compared to that of the as-cast one. No cracking is observed even at load of 1000 g implying the possibility of the limited toughness of this complex phase. Due to high hardness and high-temperature stability, this phase appears to have potential for applications as hard and tough coating materials.

✉ N. K. Mukhopadhyay
mukho.met@iitbhu.ac.in

[1] Department of Physics, Institute of Science, Banaras Hindu University, Varanasi 221005, India

[2] Department of Metallurgical Engineering, Indian Institute of Technology (Banaras Hindu University), Varanasi 221005, India

Keywords Complex metallic alloy · Laves phase · Complex intermetallics · Al-Cu-Ta system

1 Introduction

After the discovery of quasicrystals [1] in 1985, the research on complex metallic alloys (CMAs) covering a broad family of structurally complex intermetallics including quasicrystals and their crystalline approximants was intensified since the last three decades [2–9]. In general, the CMAs are understood to have a giant unit cell containing a large number of atoms up to a scale of hundreds and thousands [3–6]. The CMAs can have very unusual properties because of their large unit cell, which is no longer significant as it becomes larger than the average first-neighbour interaction similar to quasicrystals and its approximants [4–6]. Therefore, the transport of electrons and phonons cannot be observed as usual in the conventional metals and alloys. The CMAs can be classified based on the nature of the constitutive elements and their respective concentrations. Some of the complex CMAs were earlier synthesized in binary alloys, such as Na-Cd, Mg–Al and Cu-Cd [10–12] with the face-centered cubic (FCC) structure of lattice parameter, a ∼ 26.8 Å and containing around 1160 atoms in the unit cell. The description of their atomic arrangements and related interactions is really a challenging task. However, the description in terms of clusters-based approach seems to be much more convenient. These clusters are basically groups of atoms following a certain polyhedral geometry for packing. There are several phases, such as Laves phase, Frank–Kasper phase, quasicrystals and their crystalline approximants where the various kinds of clusters, e.g. tetrahedral, octahedral,

icosahedral, Mackay cluster and Berman clusters, can be identified [6, 13, 14].

The structures of CMAs can be understood based on packing of a single or several types of clusters, e.g. in Frank-Kasper phases where several clusters in the form of polyhedral packings of atoms surrounding a central atom with coordination number (CN) (or ligancy) of 12, 14, 15 and 16 can be identified. (see for example, in $Mg_{32}(AlZn)_{49}$ phase) [14–16]. Another simple example is the gamma brass structure where 52 atoms are present in the unit cell. This structural description can be simplified based on a packing of 26-atom cluster in body-cantered cubic (BCC) unit cell. This cluster is consisting of two tetrahedral, one octahedral and one cuboctahedral packings of atoms around a central atom [17, 18]. In addition, there is a simple cubic (SC) (or B2 type) gamma brass consisting of two non-identical clusters and FCC gamma brass structure consisting of 16 clusters ($16 \times 26 = 416$ atoms) in the unit cell (where $a_{FCC} = 2a_{BCC}$) can be considered as superstructure of the BCC or SC gamma brass phase.

It has been shown that the aluminium-based CMAs, which are most widely studied so far [13, 19, 20] have large unit cells with hundreds of atoms having significant amount of disorder. Recently, a series of FCC-based complex intermetallics have been reported in (AlCu)-Ta alloy systems showing the unit cells to be very large containing thousands of atoms. These structures are closely related to each other by slight change of composition. The crystal structures of such Al-Cu-Ta CMAs can be described as packing of different subsets of the clusters related to the class of Frank–Kasper phases. Because of these complexities, the mechanical and physical properties of all these phases will be interesting to study.

Three major complex phases (with stoichiometry, Pearson symbol and lattice parameter) can be mentioned here as: i) $Al_{63.6}Ta_{36.4}$, cF(444), a = 19.1663 Å; ii) $Al_{56.6}Cu_{3.9}Ta_{39.5}$, (cF(5928), a = 45.376 Å); and iii) $Al_{55.4}Cu_{5.4}Ta_{39.1}$, cF(23, 256), a = 71.490 Å [19, 20]. All these three intermetallics exhibit the same space group of $F\bar{4}3m$. It has been pointed out that these structures can be built up from the fictitious cubic Laves phase (similar to $MgCu_2$) of Al_2Ta with a lattice parameter, a = 6.5 Å. The successive phases as mentioned above can be constructed as 3x3x3 and 7x7x7 and 11x11x11 superstructures of the fictitious first order Laves phase (1x1x1). One of these higher-order phases (3x3x3) has been shown to exist in the binary Al-Ta alloy. The structure of these three higher-order superstructures can be described on the basis of various types of clusters, such as fullerenes, dodecahedra, pentagonal bifrusta and Friauf polyhedral as discussed by Steurer and co-workers [19, 20]. Ta being the high melting temperature element, the intermetallics of (AlCu)-Ta will have high-temperature strength and stability due to the complexities in the structures. It is pertinent to point out that as per earlier existing equilibrium phase diagram of Al-Ta system (Fig. 1), the existence of Al_2Ta intermetallics as a line compound has been indicated, implying its strict compositional range. However, the structure of this phase have not been evaluated properly, leading to a various conflicting result. However, Steurer and co-workers [19, 20] have shown that around $Al_{63.6}Ta_{36.4}$ composition range close to composition of Al_2Ta, a complex FCC phase (cF(444) as mentioned above can exist. The stability of this complex phase at room temperature is still open to investigation. Hence, it will be of worthy studying synthesis, structure and stability of the various intermetallic phases in (AlCu)Ta system.

In view of the above facts, in the present investigation we have selected a ternary intermetallic phase in Al-Cu-Ta system with the nominal composition of $Al_{56.6}Cu_{3.9}Ta_{39.5}$, which belongs to a family of cluster-based intermetallic phases of unprecedented complexity, containing 5928 atoms in the unit cell of 45.39 Å. The aim of the present investigation is to synthesize and characterize this phase around this composition. Even though the existence of this phase is reported in the literature, their thermal stability at high temperature and also mechanical properties have yet to be studied. Attempts will be made to ascertain whether it is a stable or metastable phase within this composition range. As this phase is based on seventh-order superstructure of Al-Ta-based Laves phase, the preliminary evaluation of mechanical properties in terms of hardness will be pursued.

2 Experimental Details

The analytical-grade aluminium (Al) granules (purity: 99.96%), tantalum (Ta) sheet (purity: 99.98%) and copper (Cu) chips (purity: 99.99%) were used for synthesis of the present alloy. All the three metals were cleaned in ultrasonic cleaning bath of acetone for 30 min. Ta sheet was cut in small rectangular pieces and mixed with Al granules, and Cu chips corresponding to $Al_{56.6}Ta_{39.5}Cu_{3.9}$ stoichiometric proportions for 5 g pellet using a digital weighing machine with 0.0001 g least count. Two pellets of $\sim$ 5 g each were prepared using a 10-cm cylindrical die by applying a pressure of $\sim 3 \times 10^5$ N/m^2 through hydraulic pressure machine. The pellet was then placed in an alumina crucible for melting in a radio frequency induction furnace (30 kW) under a continuous flow of argon gas into the silica tube. After re-melting five times, the sample was then air-cooled under argon environment within the quartz tube for 30 min. The details of the synthesis protocols are illustrated in Fig. 2. The as-cast alloy was cut into two pieces, and one piece was kept in a vacuum sealing tube

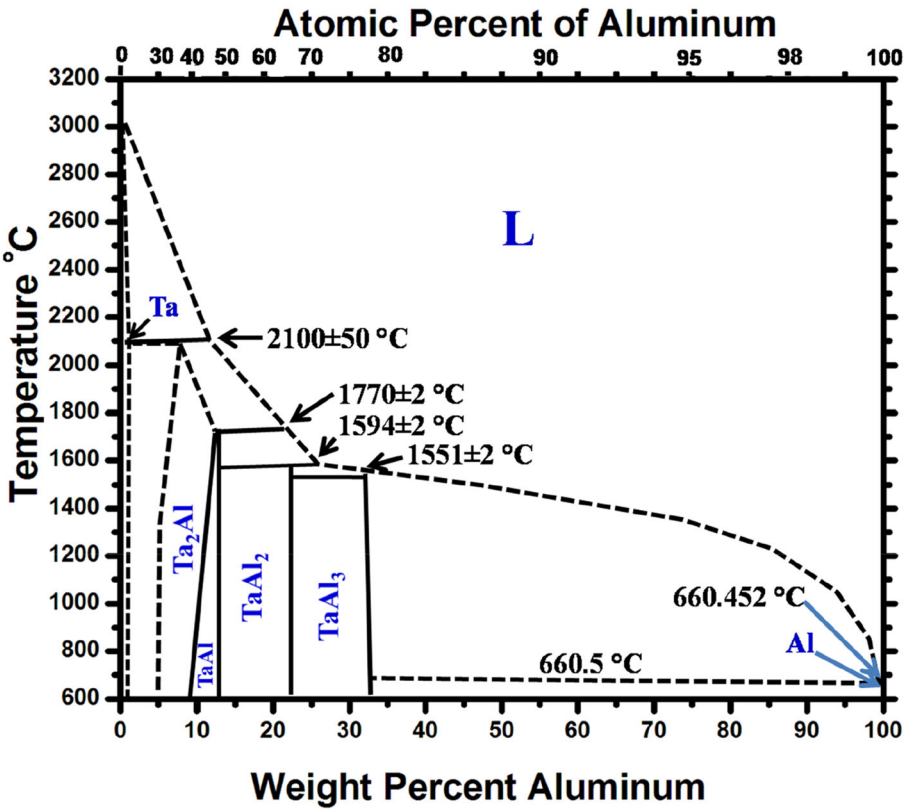

Fig. 1 HYPERLINK "sps:id::fig1|locator::gr1|MediaObject::0" Al-Ta phase diagram showing the existence of Al_2Ta line diagram intermetallic phase. The detailed crystal structure of $TaAl_2$ information is not available (ASM Handbook). However, the possibility of intermetallic phases around this composition close to fictitious Laves phase is to be noted

with 10^{-5} mbar pressure. The sealed alloy was annealed at 1400 ± 10 K for 24 h in a tubular furnace and subsequently quenched into liquid nitrogen. The powder X-ray diffraction (XRD) using the X'Pert PRO PANalytical XRD diffractometer equipped with a graphite monochromator and nickel-filtered with Cu radiation (λ = 1.5402 Å, CuKα operating at 45 kV and 40 mA) in Bragg–Brentano mode was used for structural characterization of as-cast and annealed alloys. All the measurements have been performed in the 2θ range of 10–80^0 in continuous scan mode with step size of 0.02^0 and scan step time of 1.5 s. Structural refinement of as-cast and annealed alloys was performed using Rietveld's whole profile fitting method is based on JANA2006, which is specially designed to refine simultaneously both the structural and microstructural parameters through a least square method and LeBail Fitting. The scanning electron microscope (SEM: FEI QUANTA 200) was used for surface characterization in secondary electron mode. The transmission electron microscopy (TEM: TECNAI-$20G^2$) was carried out for detailed microstructural as well as phase characterization. In order to prepare samples for TEM study, the alloys were crushed into fine powder, which was then transferred in alcohol suspension onto copper gird. An energy-dispersive X-ray spectroscopy (EDS) attached to SEM was used for elemental mapping and compositional analysis. The microhardness tester (Shimadzu) was used for hardness measurements with Vickers indenter using varying loads up to 1000 g.

3 Results and Discussion

Fine powders crushed from as-cast and annealed alloys were used for powder X-ray diffraction experiments. Figure 3 (a) shows the XRD pattern of as-cast $Al_{56.6}Ta_{39.5}Cu_{3.9}$ alloy, showing that all the diffraction peaks have been indexed based on an FCC structure with a lattice parameter, a = 45.339 (7) Å. The detailed indexing with the observed and calculated d-spacing is given in Table 1. The identification of the most intense peak as (14 14 0) type confirms the seventh-order superstructure of Al_2Ta Laves phase (corresponding to its (2 2 0) type peak). The XRD pattern of the alloy after annealing at 1400 ± 10 K

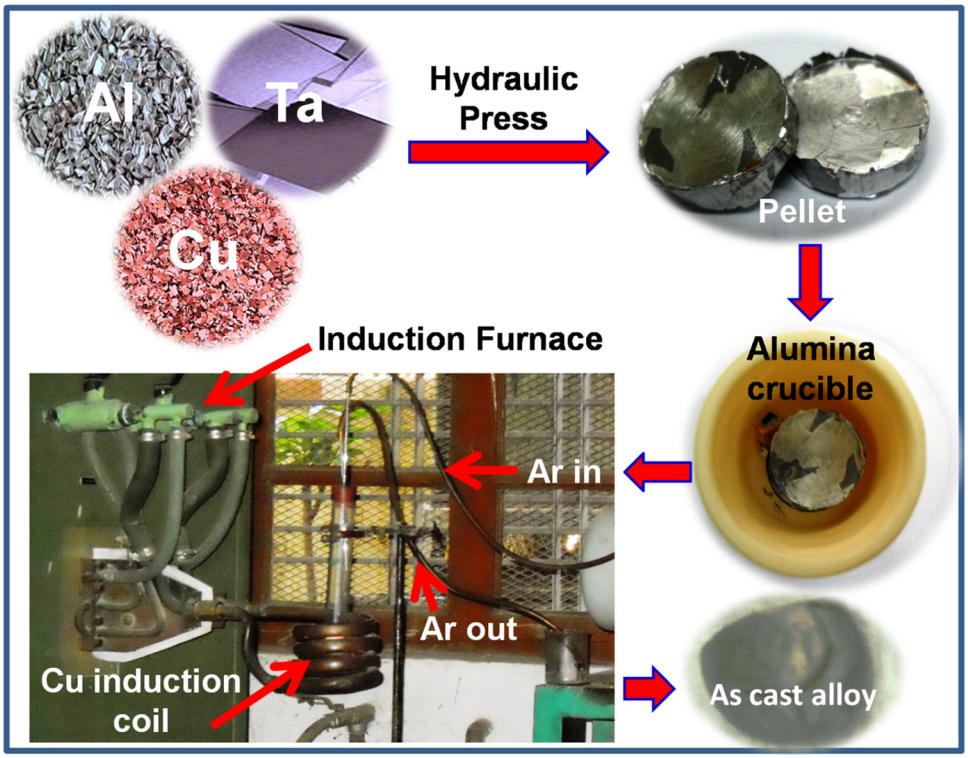

Fig. 2 Schematic diagram of synthesis protocols adopted for preparation of $Al_{56.6}Ta_{39.5}Cu_{3.9}$ intermetallics

for 24 h is shown in Fig. 3(b), and the diffraction data are displayed in Table 2. The XRD peaks are quite sharp with high intensity in the annealed alloy. There are no additional peaks; however, many peaks have vanished after annealing, *e.g.* peak observed at around $2\theta = 20.5^0$. This can be interpreted due to the evolution of recrystallized grains and the dissolution of smaller grains with other orientation. Some degree of texture in the annealed samples cannot be ruled out. The annealed alloy also conforms to the same FCC phase with a slight decrease in lattice parameter (a = 45.2908 (9) Å) based on Rietveld refinement. The overall shift of peaks from the corresponding Bragg angle is quite obvious. The Le Bail fitting of XRD patterns is shown in Fig. 3 (a, b) for the as-cast and annealed alloys. The details of fitting and other calculated parameters are shown in Table 3 and 4, respectively. For example, (14 14 0) type peak is observed at Bragg angle of 39.3563°and 39.3122° for annealed and as-cast samples, respectively (Table 1 and 2). It is obvious that the annealing has led to the reduction of lattice parameter (around 0.106%), strain relaxation, grain-coarsening, redistribution of segregated elements, elimination of the disorder (at least partially) and defects, which are being reflected from the peak sharpness and reduction of full width at half maximum (FWHM) in the annealed samples (Table 1 and 2). The chemical inhomogeneity due to non-uniform distribution of elements in the as-cast condition is always expected. The sample after prolong heat treatment can attain better chemical homogeneity in the structure. In the present case, Ta being heavier and large size atom requires more time for uniform distribution. During annealing, Ta atoms are expected to be ordered causing the reduction of lattice parameter due to shortening of the bond-length and closest atomic distances. The slightly higher lattice parameter in the as-cast materials may be due to incomplete ordering during solidification. The peak broadening observed in the as-cast alloy could be attributed to quenched-in strain and inhomogeneous chemical distribution and high degree of disorder throughout the structure. It is interesting to note that the size of defect-free domains estimated from FWHM is nearly two times higher in annealed sample compared to that in the as-cast sample, indicating that the annihilation of some defects and disorder exists in the as-cast sample.

The fractured surface of the cross-section of as-cast and annealed samples was investigated by SEM (Fig. 4 a, b). For SEM characterization, a tiny piece of the sample was removed from the bulk sample. As the sample was extremely hard, a portion of the bulk sample was fractured using a hydraulic press. Though the fractured surface could not be quantified, the features could be noted. Some granular features and cracks have been observed on the surfaces of both the alloys. The surface of the annealed sample seems to be smooth as compared to the as-cast surface, implying that the annealing has homogenized the as-cast sample. Accordingly, surface roughness decreases in the annealed sample. Though the fractured surfaces in both the cases are

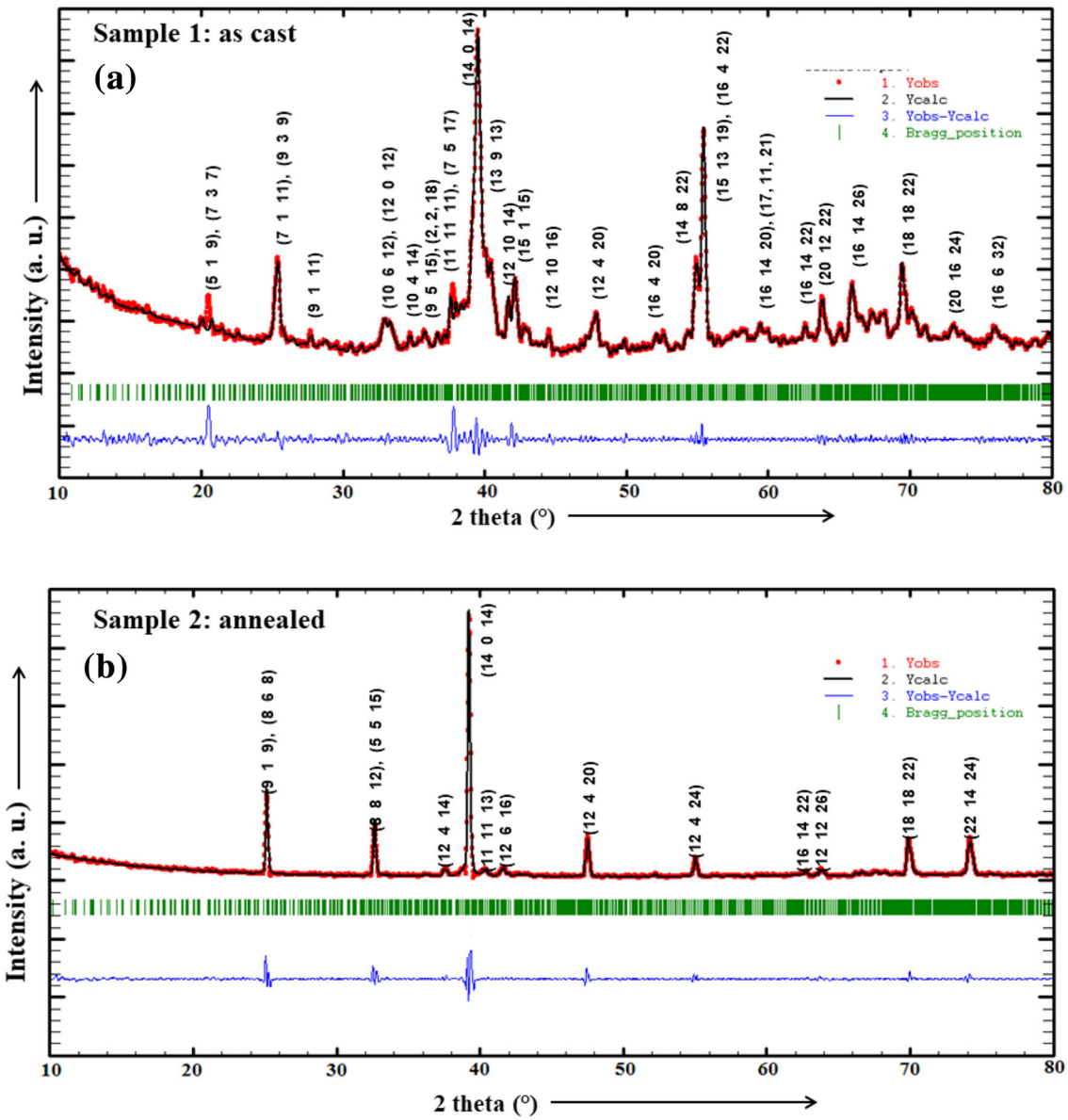

Fig. 3 The XRD patterns obtained from **a** as-cast $Al_{56.6}Ta_{39.5}Cu_{3.9}$phase and **b** after annealing 1400 k for 24 h. The calculated patterns based on Rietveld refinement have been shown. The corresponding fitting parameters and crystal structure data are displayed in Table 3 and 4 respectively; the calculated patterns have been superimposed with dotted line based on the refinement

indicative of brittle fracture, this alloy is not so brittle like ceramics, quasicrystals or glasses as it does not show any cracking under indentation load up to 1000 g. However, more investigations are required to quantify the brittleness property of such complex intermetallics. Figure 5a–c shows the colour mapping of the different elementals, *i.e.* Al, Ta, Cu which are obtained using EDS detector attached with SEM. Nearly homogeneous distribution Al, Ta and Cu in the surface of the alloy can be noticed, which lends support for homogeneous phase formation in the present experimental condition. The EDS analysis further confirms the composition of the synthesized and annealed alloy close to the stoichiometry of $Al_{56.6}Cu_{3.9}Ta_{39.5}$.

The microstructures of the as-cast and annealed samples were studied in detail by TEM. Figure 6 (a) shows a TEM bright-field image which reveals that as-cast alloy exhibits grain boundary which appears to be highly strained and this is commonly observed microstructures of the as-cast alloy. The corresponding selected area electron diffraction (SAD) pattern is shown in Fig. 6 (b) which is the typical diffraction pattern of the [111] zone axis of the FCC phase. The similar microstructure and SAD pattern have been

Table 1 Powder X-ray diffraction data obtained from as-cast sample

2 Theta (°)	FWHM (°)	Relative intensity (%)	(hkl)
20.2435	0.3317	22.5	(5 1 9), (7 3 7)
25.6725	0.3252	34.2	(7 1 11), (9 3 9)
33.0325	0.3166	15.9	(10 6 12)
33.5148	0.3161	15.9	(12 0 12), (4 4 16)
37.7727	0.3112	25.9	(11 11 11), (7 5 17)
39.3122	0.3095	100	(14 0 14)
40.7014	0.3080	32.5	(13 9 13), (9 7 17)
48.1267	0.2996	17.6	(0 0 24), (16 8 16)
55.0535	0.2919	34.3	(16 0 22), (18 4 20)
55.6566	0.2912	70.2	(15 13 19)
55.6966	0.2911	70.2	(16 4 22)
63.9674	0.2817	22.1	(6 6 30), (18 18 18)
66.1562	0.2823	26.4	(16 10 26)
69.7256	0.2866	31.7	(18 18 22)

Table 2 Powder X-ray diffraction data obtained from annealed sample

2 Theta (°)	FWHM (°)	Relative intensity (%)	(h k l)
25.0823	0.1624	31.7	(9 1 9)
25.1604	0.1625	31.7	(8 6 8), (4 2 12)
32.58	0.1666	21.5	(4 0 16), (8 8 12)
32.7642	0.1668	21.5	(5 5 15), (9 5 13)
39.3563	0.1736	100	(14 0 14)
47.4662	0.1859	17.7	(12 4 20)
54.9561	0.2011	8.7	(12 4 24)
69.8117	0.2420	15.6	(18 18 22), (14 6 30)
70.0940	0.2429	15.6	(16 10 28), (10 4 32)
74.1351	0.2568	16.1	(22 14 24), (16 10 30)
74.2729	0.2573	16.1	(10 2 34), (18 6 30)

Table 3 Lattice parameters and structural refinement parameters obtained from powder X-ray diffraction data of as-cast sample

Refined parameters and phase data	
Unit-cell parameters	a = b = c = 45.339(7) Å, $\alpha = \beta = \gamma = 90^{\circ}$
Space group	$F\bar{4}3m$ (Space Group = 216)
R-factor	R_p = 3.81%, $_wR_p$ = 6.08%, GOF = 0.82%,
Volume	V = 93,183.2 $Å^3$

observed in the annealed sample (Fig. 6 c, d), respectively. However, the SAD pattern from annealed samples appears to have sharper peaks and can be identified as [111] zone axis, indicating more ordering in the annealed alloy. The diffuse scattering associated with diffraction patterns can be observed. More detailed investigation is required to understand the origin of diffuse scattering and also the contrast in the images in order to correlate with the various

Table 4 Lattice parameters and structural refinement parameters obtained from powder X-ray diffraction data of annealed sample

Refined parameters and phase data	
Unit-cell parameters	a = b = c = 45.2908(9) Å, α = β = γ = 90̊
Space group	$F\bar{4}3m$ (Space Group = 216)
R-factor	R_p = 7.63%, $_wR_p$ = 13.73%, GOF = 0.55%,
Volume	V = 92,909.6 $Å^3$

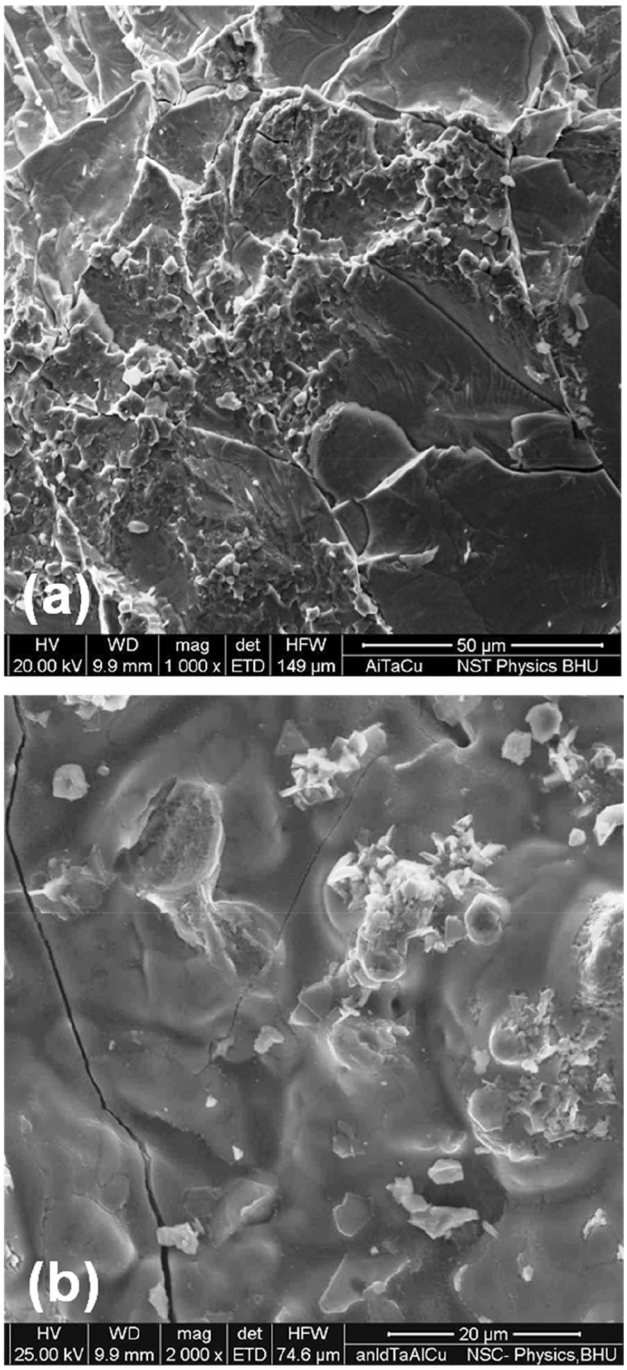

Fig. 4 The SEM fractography of **a** as-cast and **b** annealed samples showing the brittle fracture and also surface cracks

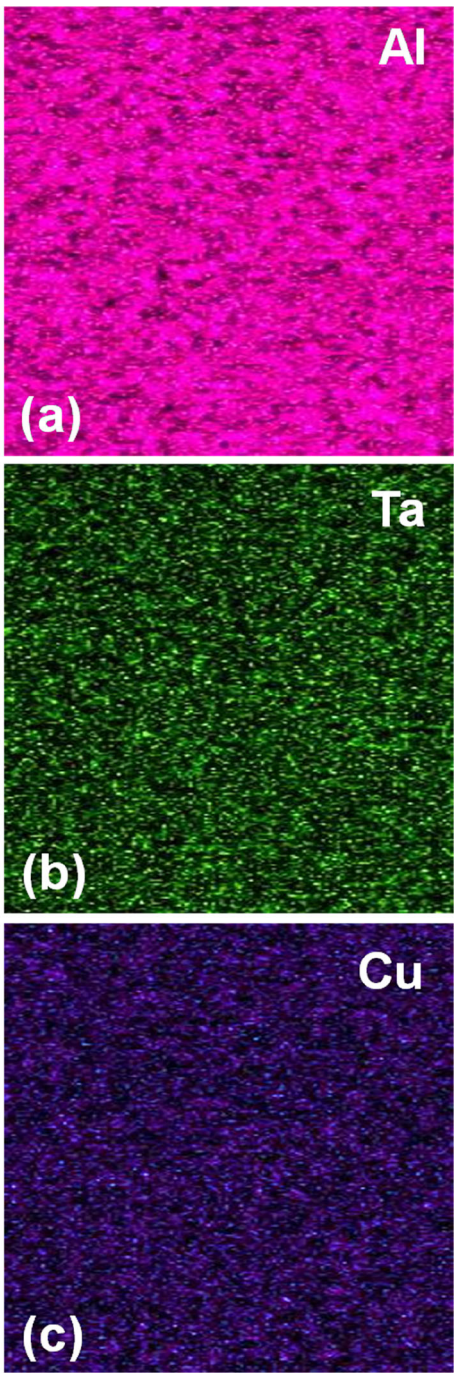

Fig. 5 The EDS colour mapping of the annealed $Al_{56.6}Ta_{39.5}Cu_{3.9}$ phase showing the uniform distribution of the elements

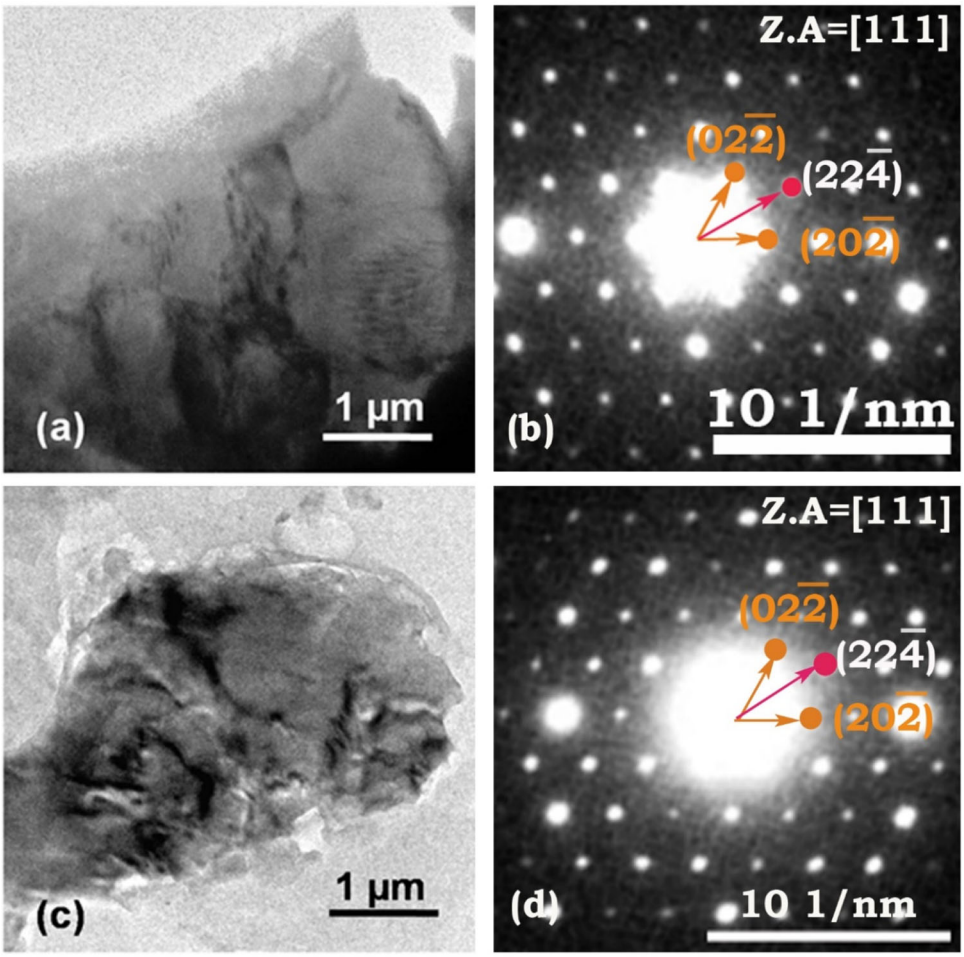

Fig. 6 **a** TEM bright-field image of as-cast $Al_{56.6}Ta_{39.5}Cu_{3.9}$ sample and **b** corresponding selected area electron diffraction pattern, **c** bright-field image of annealed sample, **d** corresponding selected area electron diffraction pattern. The diffraction patterns show the zone axis along [111] and are consistent with observation of FCC phase in XRD patterns

defects and disorder that could be inherent part of this kind of complex structures. The SAD results are in close agreement with the XRD results of corresponding alloys.

The as-cast and annealed samples were prepared for hardness testing by polishing the surface using Al_2O_3 powder. The hardness tests, conducted from 10 to 1000 g load, indicate the variation of hardness with load. The average microhardness is found to vary from 8.8 GPa to 7.2 GPa for annealed sample and 7.6 GPa to 4.8 GPa for as-cast samples (Fig. 7). The variation of hardness with load is known as indentation size effect (ISE), which is found to be existing in the present alloys. In the case of as-cast sample, the variation is quite significant compared to that of the annealed sample. The ISE is almost insignificant at the load higher than 100 g. The bulk hardness which is independent of load can be accepted as true representative of the characteristic mechanical property of the material. In the present alloys, average hardness can be considered to be 7.2GPa, whereas the same for as-cast sample is around 4. 8 GPa. It is important to point out that no cracks have been detected during the indentation tests even at 1000 g load. It supports the idea that this intermetallic phase

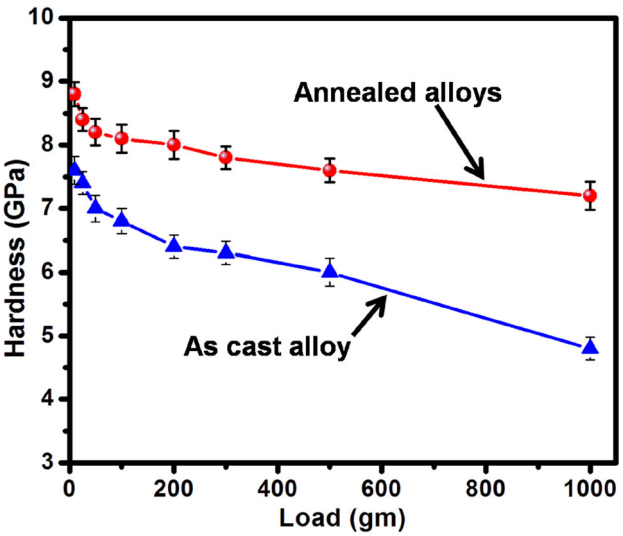

Fig. 7 Variation of microhardness (GPa) with load from 10 to 1000 g displayed for the as-cast $Al_{56.6}Ta_{39.5}Cu_{3.9}$ and annealed samples. The indentation size effect can be deciphered. The hardness varies from 8.8(at 10 g) to 7.2 GP (at 1000 g) in the case of annealed sample, whereas in as-cast sample, it varies from 7.6 GPa to 4.8GPa

though complex is not as brittle as any other intermetallics, ceramic and quasicrystals as well as glasses of comparable hardness [21]. At lower load, it requires more stress to generate geometrically necessary dislocations (GNDs) and gives rise to higher hardness as suggested by the theory of strain gradient plasticity. In the as-cast materials, the chemical inhomogeneity could be one of the reasons for overall lower hardness. It should be emphasized that the average hardness of this intermetallic is quite high and comparable to martensitic or high-strength steel, but at the same time it is not as brittle unlike other complex intermetallics. The ductile nature of all the FCC alloying elements, as well as a large amount of intrinsic disorder in their FCC structure, may be responsible for their relatively higher toughness. However, more studies are required to understand the origin of toughness and deformation behaviour. Due to its high strength and reasonable toughness, the present intermetallic phase seems to have potential for developing as suitable coating materials on soft Al-alloys.

It is clear that the as-cast alloy in the present experimental condition does not lead to any phase transformation during annealing, implying that this phase is relatively stable at this composition. It has been mentioned earlier that no Laves phase of first order has been reported in Al-Ta alloy system as either stable or metastable form. It may be understood due to the fact that there is a geometrical requirement of size ratio of the bigger and smaller atoms (R_L/R_S) in the range of 1.225for formation of perfect structure of Laves phase. But in the case of Al-Ta system, the atomic size of both Al and Ta appears to be similar (R = 1.43 Å). Hence in the binary alloy, the Laves phase is not likely to be stabilized due to the requirement of geometrical constraints. However, by adopting non-equilibrium processing technique, it would be possible to obtain metastable Laves phase, which may be explored further. The addition of Cu might be providing the additional stability of the higher-order superstructure of Laves phase. Following semi-empirical model, it has been calculated that the mixing enthalpy of Al-Ta is highly negative (around -20 kJ/mole), which also explains why the solid solubility cannot be expected though the atomic radius is found to be similar. In addition, we can look at the valence electron factor also, which for Ta (with $4f^3 5s^2$configuration) and Al (with $3s^2$ $3p^1$ configuration) can be estimated to be 5 and 3, respectively. Thus, the valance electron concentration (*i.e.* electron per atom, e/a) seems to be not favourable for solid solution formation with unsaturated 4f subshell of Ta. Hence, solid solution or simple type of Laves phase is also not formed or stabilized. However, by changing the chemistry, *e.g.* by addition of Cu atom perhaps it can lead to the formation of higher-order Laves phase as reported [19, 20]. Recently, Okamoto [22] has advocated a new Al-Ta phase diagram (different from Fig. 1) by taking into account the earlier data as well as the latest experimental and theoretical data reported by Witusiewicz et al. [23]. It has been shown that the $Al_{69}Ta_{39}$binary intermetallic phase does exist at higher temperature but not at room temperature. This may be noted that this stoichiometry as $Al_{69}Ta_{39}$ is close to $Al_{63.6}Ta_{36.4}$ (at%) investigated by Weber et al. [19] and Conrad et al. [20] revealing correlation with the third-order superstructure of Laves phase. However, the confusion still exists whether the intermetallic phases around this composition of Al_2Ta are stable or metastable at room temperature. Therefore, more investigations are warranted to explore the range of composition and the structural stability of various intermetallic phases around this composition close to Al_2Ta in binary or ternary alloy, i.e. $(AlCu)_2Ta$, which is not yet clearly settled. It can be intuitively understood that the complex phases with giant unit cell and close packing configuration do possess high degree disorder in the structures. Hence, the deformation in terms of dislocation activity will also be of interest to study further for potential technological applications.

4 Conclusions

We have successfully synthesized a complex intermetallics close to $Al_{56.6}Cu_{3.9}$ $Ta_{39.5}$ composition by induction melting under controlled atmosphere. From XRD data followed by Rietveld refinement, it was established that an intermetallic phase conforming to the space group, F $\overline{4}$ 3 m (SG: 216) with lattice parameter, a = 45.339 (7) Å and a = 45.2908 (9) Å have been formed in as-cast and annealed samples, respectively. This complex intermetallic phase has been correlated with the seventh order superstructure of Al_2Ta fictitious Laves phase (as it is not yet observed to exist) around this composition. The reduction of lattice parameter is observed in the case of annealed sample, and it has been attributed to the ordering and homogeneous distribution of alloying elements, especially Ta. The electron diffraction patterns obtained from both the samples are in close agreement with the observation of XRD data. The indentation behaviour has been analysed, and ISE has been attributed to the strain gradient plasticity as this alloy shows limited ductility and it has not shown any cracking even at higher load of 1000 g. The average microhardness is found to vary from 8.8GPa to 7.2GPa for annealed samples and 7.6 GPa to 4.8 GPa for as-cast samples implying the existence of indentation size effect which can be qualitatively attributed to strain gradient plasticity. No cracking observed during indentation event suggests its better toughness compared to quasicrystals, other intermetallics and glasses of comparable hardness. More investigation is required to understand the

deformation and stability at room and relatively higher temperature around this composition for application as coating materials on soft metallic surfaces.

Acknowledgements Authors would like to thank (Late) Prof. O.N. Srivastava and also Prof. S. Lele, Prof. R.S. Tiwari, Prof. R.K. Mandal, Prof. B.N. Sarma, Dr. Vivek Pandey, Dr. Yagnesh Shadangi, Mr Rajendra Prasad and Mr. Saptarshi Mukherjee for many useful discussions. TPY thanks the University Grants Commission (UGC) (Grant No. F5-154/2016(IC)), India, for carrying out this work. NKM would like to acknowledge the support of the Department of Science and Technology (DST), Government of India, under the scheme of 'Fund for the Improvement of S&T Infrastructure' (FIST) (Grant No TPN 32537) for providing necessary facilities for electron microscopy analysis.

Author's contributions TPY was involved in experimental design, conceptualization, writing—original draft, formal analysis, data curation, writing-review and editing. HA was involved in Formal analysis and Rietveld refinement of X-ray diffraction data. MAS was involved in editing. NKM was involved in conceptualization, writing-original draft, formal analysis, data curation, writing—review and editing.

Declarations

Conflict of interest The authors declared that there is no conflict of interest.

References

1. Shechtman D, Blech I, Gratias D and Cahn J W, *Phys. Rev. Lett.,53*(1984) 1951.
2. Chattopadhyay K, Lele S, Ranganathan S, SubbannaGN and Thangaraj N, *Current Science*, **54** (1985) 895.
3. Urban K and Feuerbacher M, *Journal of Non-Crystalline Solids*, **334–335** (2004) 143.
4. Dubois JM, Ferre EB and Feuerbacher M, *Complex Metallic Alloys: Fundamentals and Applications*(ed) Dubois J M and Belin-FerréE, WILEY-VCH Verlag GmbH & Co. KGaA, Weinheim(2011) p 1–39 ISBN: 978–3–527–32523–8.
5. Dubois JM,*Chemical Society Reviews*, **41** (2012) 6760.
6. Yadav T P, Tiwari RS and Srivastava ON,*Journal of non-crystalline solids* 334-335 (2004) 39.
7. Mukhopadhyay N K, IshiharaK N, Ranganathan Sand ChattopadhyayK, *Acta Metall. Mater*.,**39** (1991) 1151.
8. MukhopadhyayNK and YadavTP, *Isr. J. Chem.*, **51** (2011) 1185.
9. YadavTPand MukhopadhyayN K, *Current Opinion in Chemical Engineering,19* (2018) 163.
10. Samson S, *Nature*, **195** (1962) 259.
11. Samson S,*Acta Cryst.19* (1965) 401.
12. Samson S, *Acta Cryst*., **23**, (1967) 586.
13. Dshemuchadse J, Jung D Yand Steurer W, *Acta Cryst.*B**67** (2011) 269.
14. MukhopadhyayN K, Chattopadhyay K and RanganathanS, *Metallurgical Transactions A*, **20** (1989) 805.
15. Frank FC and KasperJ S, *Acta Cryst.11* (1958) 184.
16. Frank F C and KasperJ S, *ActaCryst11* (1959) 483.
17. MukhopadhyayNK, MukherjeeD, BeraS, MannaI and MannaR, *J Mater. Sci. &Engg. A*, **485** (2008) 673.
18. MukhopadhyayNK, MukherjeeD, DuttaS, MannaR, KimDH and MannaI, *Journal of Alloys and compounds,457* (2008) 177.
19. Weber T, Dshemuchadse J, Kobas M, Conrad M, Harbrecht B and Steurer W,*Acta Cryst.B65* (2009) 308.
20. Conrad M, Harbrecht B, Weber T, Jung D Y andSteurer W,*ActaCryst.B65* (2009) 318.
21. Mukhopadhyay N Kand PauflerP, *International Materials Reviews,* **51** (2006) 209.
22. Okamoto H, *Journal of Phase Equilibria and Diffusion*, **31** (2010) 578.
23. WitusiewiczV T, BondarA A, HechtU, ZollingerJ, PetyukhVM, FomichovOS, VoblikovVM and RexS, *Intermetallics,* **18** (2010) 92.